U.P.B. Sci. Bull., Series D, Vol. 83, Iss. 4, 2021 ISSN 1454-2358

A MODEL OF DYNAMIC VIBRATIONS ABSORBER FOR A HELICOPTER

Félix TIPHAINE[1], Mihai Valentin PREDOI[2]

Reducing helicopter vibrations is a constant preoccupation of the last decades. Most important is to reduce the vibrations produced by the main rotor rear in the cabin. The use of vibrations dampers is a possible solution, but a vibration absorber is more efficient by the vibrations of a secondary system close to its resonance. In this way, vibration energy from the principal system, the helicopter in this case, is partly absorbed by the vibration damper.

In this paper is investigated a special kinematic link for a vibration absorber. The mechanical model, Lagrange equations of the non-holonomic system are deduced and the numerical results are validated by experimental tests on a laboratory model.

Keywords: Dynamic Vibration Absorber, non-holonomic system.

1. Introduction

High level of vibrations and associated noise, represent a constant preoccupation in helicopter design, just to mention one of many technical domains in which vibration reduction is very important. The principal source of vibrations in the helicopter case is the transmission gearbox which reduces the rotation speed of about $(3 - 20)\cdot 10^3$ rot/min from the free turbine of the engine, to 300 - 1000 rot/min of the main rotor, providing power to the main rotor propeller, ranging from hundreds to thousands of kilowatts.

The main gearbox vibrations are transmitted to the helicopter cabin through the connection joints, which must be sufficiently stiff to carry the helicopter weight and payload. Reducing these vibrations, preferably near their source, is a constant preoccupation in modern design of helicopters. Two theoretical directions of study can be distinguished: one consisting in adding vibrations dampers and the other considers the vibrations absorbers. The two degrees of freedom forced and damped vibrations are extensively presented in classical textbooks e.g. [1], [2], [3], etc. A dynamic vibration absorber is a tuned spring-mass system, which reduces or

[1] Master Student, Faculty of Aerospace Engineering, University POLITEHNICA of Bucharest & Arts et Métiers Institute of Technology, Cluny, France, e-mail: felix.tiphaine@ensam.eu
[2] Prof., Dept. of Mechanics, University POLITEHNICA of Bucharest, Romania, e-mail: mihai.predoi@upb.ro

eliminates the vibration of a harmonically excited system. Fundamental aspects concerning the vibrations absorbers can be found in textbooks e.g. [2], [4], [5], etc.

More recently Yuen et al. [6] are focusing on the design and implementation of passive vibration absorbers for machines with a known vibration frequency close to one of the system resonance frequencies, taken as example a cantilever beam. The limits of the added device when the vibration absorber is not tuned are clearly shown. Piccirillo et al. [7] are proposing a new procedure to determine the optimal parameters of a *Dynamic Vibration Absorber* (DVA), considering both damped and undamped primary system. Shen et al [8] studied in detail a novel DVA with grounded stiffness element and amplifying mechanism. Some helicopter specific vibrations problems are presented by C. -Rivera and T. -Rodriguez in ref. [9] and in the dedicated chapter in the textbook [10] edited by Concilio et al. Simpler mechanisms have been studied in many papers, citing here only Ji et al. [11] and Nguyen et al. [12].

The present work is investigating a mathematical model of helicopter dynamic structure, simplified to a mechanical system with a small number of degrees of freedom. The DVA is considered as a beam connecting the cabin structure to the main gearbox, a beam which can have a relative motion and a mass positioned near its free end. The energy loss is caused by two mechanisms: a) structural loss in the elastic parts or viscous dampers and b) friction in the slider connecting the beam to the gearbox. The work is organized as follows: a) the mathematical model deduced from Lagrange equations, b) numerical simulation of the dynamic response of the structure, c) preliminary experimental validation.

2. Mechanical model

The mechanical model is intended to capture only the vertical translations of the cabin and main gear, including also a simplified model of the DVA (Fig. 1).

The mass of the fuselage (cabin and landing gear) are represented by the mass M_f positioned by z_f, small amplitude vibrations about the equilibrium position. The contact with the ground (suspension and wheels) are modeled by the spring elastic constant k_f and damper c_f. The gear box and main rotor are represented by the mass M_g positioned by the absolute coordinate z_g, from its equilibrium position. Between the cabin and the gearbox, are the mechanical links represented by the elastic spring of constant k_g and viscous damper of constant c_g. The DVA is represented by the beam CB of length L and negligible mass, passing through a slider which is hinged in A to the gearbox. At point B is attached a mass M_b. The beam is inclined at an angle α_0 at equilibrium and small variations of this angle are denoted by $\alpha(t)$. Of course in reality, for equilibrium reasons, several DVAs will be symmetrically distributed around the main rotor, as well as the springs and dampers included in this model, meaning a sum of masses and an equivalent spring, to be updated.

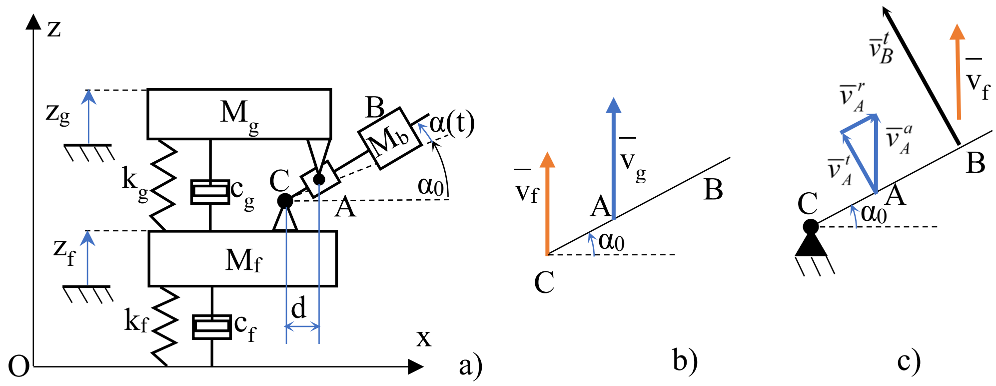

Fig. 1 Mechanical model of the cabin-gearbox assembly with the DVA included (a). Kinematic physical parameters (b). Equivalent velocities in a translating frame (c).

The beam CB is in a planar motion. The position of the DVA mass M_b can be deduced from the following kinematic analysis (Fig. 1 b). Points C and A have absolute velocities $\dot{z}_f$ and $\dot{z}_g$ respectively, along the vertical direction Oz. The segment *CA(t)* has a constant projection on the horizontal direction Ox (Fig. 1): $d = CA(t)\cdot\cos\left[\alpha_0+\alpha(t)\right] \cong CA(t)\cdot\cos(\alpha_0)$. Considering the entire system as in a moving frame of velocity $\dot{z}_f$, the problem is reduced to the relative motion of the slider A (Fig. 1c). In this frame:

$$\left|\bar{v}_A^a\right| = \dot{z}_g - \dot{z}_f$$
$$\left|\bar{v}_A^t\right| = \left|\bar{v}_A^a\right|\cos(\alpha_0+\alpha) = \dot{\alpha}\cdot CA(t) = \dot{\alpha}\cdot\frac{d}{\cos(\alpha_0+\alpha)} \tag{1}$$

Consequently, the angular velocity of the beam, could be written by keeping terms up of order $O(\alpha^2)$ in a series development around α_0, but a simpler approximation will be used in the following, to avoid non-linear terms:

$$\dot{\alpha} = \frac{\dot{z}_g - \dot{z}_f}{d}\left(\cos^2\alpha_0 + \alpha\sin 2\alpha_0 + O(\alpha^2)\right) \cong \frac{\dot{z}_g - \dot{z}_f}{d}\cos^2\alpha_0 \tag{2}$$

The point B has an absolute velocity in the fixed frame, given by the rotation in the translating frame and by the overall translation velocity $\dot{z}_f$:

$$v_{Bx} = -L\dot{\alpha}\cdot\sin(\alpha_0+\alpha) \cong -L\dot{\alpha}\cdot\sin\alpha_0$$
$$v_{Bz} = \dot{z}_f + L\dot{\alpha}\cos(\alpha_0+\alpha) \cong \dot{z}_f + L\dot{\alpha}\cos\alpha_0 \tag{3}$$

Using the notation:

$$\lambda = (CB/d)\cos\alpha_0 = (L/d)\cos\alpha_0, \tag{4}$$

the velocity becomes a linear combination of the two absolute velocities and $\lambda = L/d$ if the beam's inclination angle α_0 is small, can be obtained the preliminary results from ref. [13]:

$$v_{Bx} \cong 0$$
$$v_{Bz} \cong \dot{z}_f(t) + \lambda(\dot{z}_g - \dot{z}_f) = \lambda\dot{z}_g + (1-\lambda)\dot{z}_f \tag{5}$$

In the general case of angle $\alpha_0 \in (0, \pi/2)$ and small angles α, one can limit the v_B^2 from (3), to only the first two terms of the series development :

$$v_B^2 = \dot{z}_f^2 + L^2\dot{\alpha}^2 + 2L\dot{z}_f\dot{\alpha}\cos(\alpha_0+\alpha)$$
$$= \dot{z}_f^2 + L^2\dot{\alpha}^2 + 2L\dot{z}_f\dot{\alpha}\cos\alpha_0 - 2L\dot{z}_f\alpha\dot{\alpha}\sin\alpha_0 + \mathrm{O}(\alpha^2) \tag{6}$$

The kinetic energy of the mechanical system is, for small angle α, neglecting the last term of the velocity (6), or directly from the approximate form of (3):

$$E = \frac{1}{2}M_f\dot{z}_f^2 + \frac{1}{2}M_g\dot{z}_g^2 + \frac{1}{2}M_b v_B^2$$
$$= \frac{1}{2}\left[(M_f+M_b)\dot{z}_f^2 + M_g\dot{z}_g^2 + M_b L\dot{\alpha}(L\dot{\alpha} + 2\dot{z}_f\cos\alpha_0)\right]. \tag{7}$$

Apparently, there are three generalized velocities involved in this formula. However there is a relationship (2) between them, meaning that the mechanical system has only two degrees of freedom. Being a relationship expressed in velocities, the system can be treated as non-holonomic. The forces considered as acting on the mechanical system are the weights, elastic forces in the springs for which there is a force function, defined up to an additive constant C:

$$U = -M_f g z_f - M_g g z_g - M_b g\left(z_f + L\sin(\alpha_0+\alpha)\right) - \frac{1}{2}k_f z_f^2 - \frac{1}{2}k_g(z_g - z_f)^2 + C\,. \tag{8}$$

For small α angles, a Taylor series development can be written up to terms in α of second order:

$$U=-g\left\{M_f z_f+M_g z_g+M_b\left[z_f+L\left(\sin\alpha_0+\frac{\cos\alpha_0}{1!}\alpha-\frac{\sin\alpha_0}{2!}\alpha^2\right)\right]\right\}-\frac{1}{2}\left[k_f z_f^2+k_g\left(z_g-z_f\right)^2\right]+C \tag{9}$$

By derivation of this force function about the generalized coordinates z_f, z_g, α will result constant forces and forces depending on coordinates. The first group:

$$U_s=-M_f g z_f-M_g g z_g-M_b g\left(z_f+L\left(\sin\alpha_0+\frac{\cos\alpha_0}{1!}\alpha\right)\right). \tag{10}$$

leads to particular solutions of the Lagrange equations, corresponding to the equilibrium position, which do not influence the vibrations. Consequently, only the dynamic force function will be considered in the following:

$$U=-\frac{1}{2}k_f z_f^2-\frac{1}{2}k_g\left(z_g-z_f\right)^2+M_b g L\frac{\sin\alpha_0}{2}\alpha^2+C. \tag{11}$$

Also, the viscous damping forces defined by damping coefficients c_f, c_g and the external applied forces e.g. $F(t)$ produce generalized forces :

$$Q_f=-c_f\dot{z}_f;\ \ Q_g=-c_g\left(\dot{z}_g-\dot{z}_f\right)+F(t). \tag{12}$$

3. The Lagrange equations

In the case of non-holonomic Lagrange equations, the equation (2) relating the three generalized velocities ($\dot{z}_f, \dot{z}_g, \dot{\alpha}$) will be included, by using the Lagrange multiplier β for the single kinematic constraint:

$$\begin{aligned}&\frac{d}{dt}\left(\frac{\partial E}{\partial \dot{q}_k}\right)-\frac{\partial E}{\partial q_k}=\frac{\partial U}{\partial q_k}+Q_k+\beta a_k;\ \ k=1,2,3\\&-\dot{z}_f+\dot{z}_g-\frac{d}{\cos^2\alpha_0}\dot{\alpha}=0\ \Rightarrow a_1=-1;\ a_2=1;\ a_3=-\frac{d}{\cos^2\alpha_0};\end{aligned} \tag{13}$$

Consequently, the Lagrange equations and associated kinematic condition, are in this case:

$$\begin{cases} \left(M_f + M_b\right)\ddot{z}_f + M_b L\ddot{\alpha}\cos\alpha_0 + k_f z_f - k_g\left(z_g - z_f\right) + c_f\dot{z}_f - \beta = 0; \\ M_g\ddot{z}_g + k_g\left(z_g - z_f\right) + c_g\left(\dot{z}_g - \dot{z}_f\right) + \beta = 0; \\ M_b L\left(L\ddot{\alpha} + \ddot{z}_f\cos\alpha_0 - \alpha g\sin\alpha_0\right) - \beta\dfrac{d}{\cos^2\alpha_0} = 0; \\ \dot{z}_g - \dot{z}_f - \dfrac{d}{\cos^2\alpha_0}\dot{\alpha} = 0. \end{cases} \tag{14}$$

The derivative of the kinematic condition with respect to time, permit the elimination of the angular generalized coordinate and from the third equation is deduced β, injected then in the first and second equation:

$$\begin{cases} \ddot{\alpha} = \dfrac{\cos^2\alpha_0}{d}\left(\ddot{z}_g - \ddot{z}_f\right) \\ \beta = M_b\lambda\cos\alpha_0\left(L\ddot{\alpha} + \ddot{z}_f\cos\alpha_0 - \alpha g\sin\alpha_0\right) \\ = M_b\lambda\cos^2\alpha_0\left(\left(1-\lambda\right)\ddot{z}_f + \lambda\ddot{z}_g + g\dfrac{z_f - z_g}{2d}\sin 2\alpha_0\right) \end{cases} \tag{15}$$

Since only the vertical vibrations are of interest in this analysis, eq. (15) will be used to express the system of differential equations (14) to one only two . The resulting Lagrange equations in matrix form, including the action of an external force *F(t)* acting on the gear-box are:

$$\begin{gathered} \begin{bmatrix} m_{11} & m_{12} \\ m_{21} & m_{22} \end{bmatrix}\begin{Bmatrix} \ddot{z}_g \\ \ddot{z}_f \end{Bmatrix} + \begin{bmatrix} c_{11} & c_{12} \\ c_{21} & c_{22} \end{bmatrix}\begin{Bmatrix} \dot{z}_g \\ \dot{z}_f \end{Bmatrix} + \begin{bmatrix} k_{11} & k_{12} \\ k_{21} & k_{22} \end{bmatrix}\begin{Bmatrix} z_g \\ z_f \end{Bmatrix} = \begin{Bmatrix} F(t) \\ 0 \end{Bmatrix} \\ m_{11} = M_g + M_b\lambda_0\lambda; \quad m_{12} = M_b\lambda_0\left(1-\lambda\right); \\ m_{21} = m_{12}; \quad m_{22} = M_f + M_b\left[1 - \lambda_0\left(2-\lambda\right)\right]; \\ c_{11} = c_g;\ c_{12} = -c_g;\ c_{21} = 0;\ c_{22} = c_f; \\ k_{11} = k_g - M_b\lambda_0 g\dfrac{\sin 2\alpha_0}{2d}; \quad k_{12} = -k_g + M_b\lambda_0 g\dfrac{\sin 2\alpha_0}{2d}; \\ k_{21} = k_{12}; \quad k_{22} = k_f + k_g - M_b\lambda_0 g\dfrac{\sin 2\alpha_0}{2d}. \end{gathered} \tag{16}$$

The notation $\lambda_0 = \lambda\cos^2\alpha_0$ has been used. The above differential equation are extending the results from ref. [13] to the case of arbitrary inclination α_0 of the DVA.

4. Natural frequencies

The resonance in real conditions occurs as high vibration amplitudes at some particular frequencies of the damped system. Since in laboratory conditions, the damping coefficients are a priori unknown, the next step is to determine the natural frequencies using the measured physical quantities of an experimental model. The angular frequencies $\omega_{1,2}$ (rad/s) can be obtained numerically by solving the following eigenvalue problem:

$$-\omega^2\begin{bmatrix} m_{11} & m_{12} \\ m_{21} & m_{22} \end{bmatrix}\begin{Bmatrix} z_g \\ z_f \end{Bmatrix}+\begin{bmatrix} k_{11} & k_{12} \\ k_{21} & k_{22} \end{bmatrix}\begin{Bmatrix} z_g \\ z_f \end{Bmatrix}=\begin{Bmatrix} 0 \\ 0 \end{Bmatrix} . \tag{17}$$

The resonant frequencies depend on the design parameters L/d =1… 10 and $\alpha_0 = 0 \ldots \pi/3$ from which are deduced the parameters (λ, λ_0) used in the previous paragraph. The input values were determined on the reduced scale model used in laboratory (Table 1). In Fig. 2 are shown these dependencies.

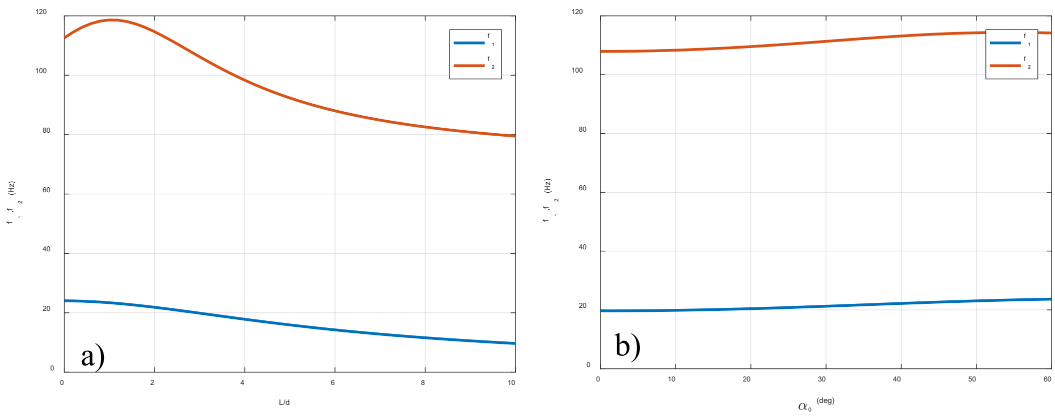

Fig. 2 Natural frequencies as functions of L/d and α_0 = 26 ° (a) and as functions of α_0 for L/d=5

In the absence of added mass (M_b=0) the computed natural frequencies are f_1=24.05 Hz and f_2=120.22 Hz. The essence of the DVA is to add the Mb masses indicated in Table 1. The experimental α_0 = 26° and this value was kept constant while changing the ratio L/d with the results shown on Fig. 2a. Placing the mass farther from the hinge, reduces considerably the fundamental frequency from 24.05 Hz to 9.7 Hz, approaching it to usual rotation frequencies of real main helicopter rotors. This means that the DVA is tunable to the frequency of the rotor. The second frequency increases from 112.5 Hz at L/d=0, up to 118.6 Hz for L/d=1 and diminishes to 80 Hz for L/d=10.

5. Dynamic response of the DVA

The most intense vibrations in a helicopter are produced by the main rotor and these can be considered as harmonic excitations as shown by the equations (16). In our case, the harmonic excitation is produced by two variable speed electric motors, up to 170 rot/min. Consequently the excitation force can be written as $F(t) = m_u r_u \Omega^2 = u\Omega^2$ in which the unbalance coupled with periodic plateau motion along the vertical direction are denoted u, which in our experimental model would correspond to the product of the unbalanced mass m_u and the radial position of this unbalance r_u. The value for u can only be estimated and after computations, can be adjusted to fit the experimental results. However, acceptable values depend on the mass of the wheels and their possible eccentricity, and is estimated to a maximum value of 100 g.mm. The dynamic response system of equations resulting form eq. (16) is thus written in displacements amplitudes A_g and A_f respectively:

$$\begin{bmatrix} k_{11} + i\omega c_g - \omega^2 m_{11} & k_{12} - i\omega c_g - \omega^2 m_{12} \\ k_{21} - \omega^2 m_{21} & k_{22} + i\omega c_f - \omega^2 m_{22} \end{bmatrix} \begin{Bmatrix} A_g \\ A_f \end{Bmatrix} = \Omega^2 \begin{Bmatrix} u \\ 0 \end{Bmatrix} \qquad (18)$$

The damping coefficients c_g, c_f are estimated parameters of the dynamic response, remaining to be corrected after experimental tests. The influence of the *L/d* ratio for low damping $c_g = c_f = 10$ Ns/m is shown for $\alpha_0 = 26°$ on Fig. 3.

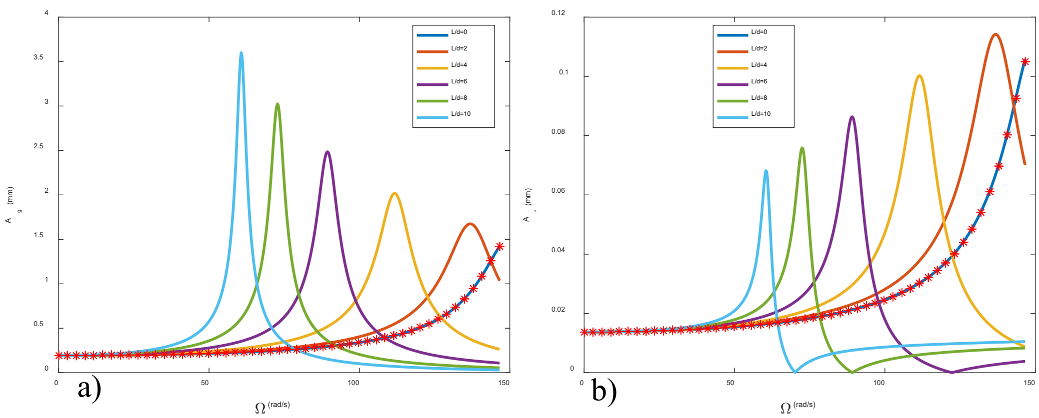

Fig. 3 Displacement amplitude of the gearbox (a) and of the fuselage (b) for low damping. (*) : without DVA.

The weak damping leads to expected high amplitudes at the "quasi-resonances" for both the gearbox and the fuselage, compared to the static deformations. Even in this case however, the DVA effect is obvious for the fuselage, as shown by the frequencies at which the vibration amplitude drops to zero and remains very low at higher frequencies. The lowest DVA active frequency is at 70 rad/s (11.1Hz) for L/d =10. Usually in such configurations are installed more efficient dampers, e.g. *cg*= *cf* = 150 Ns/m.

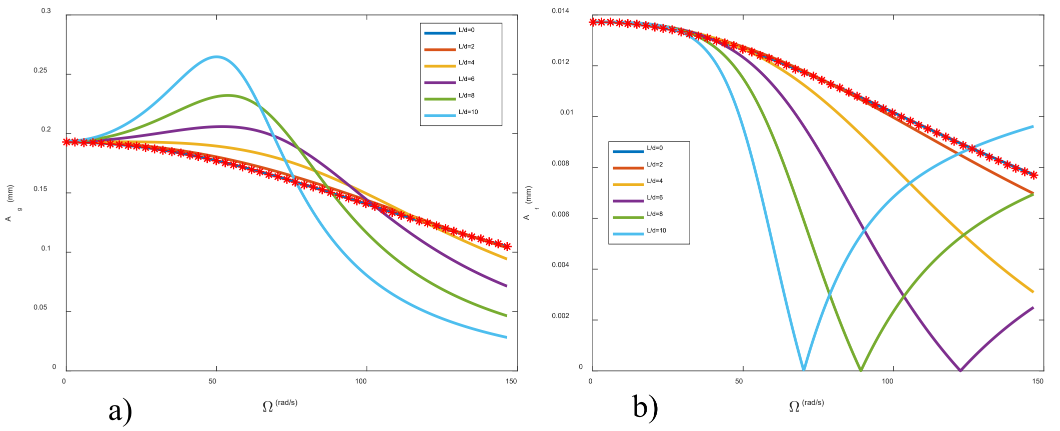

Fig. 4 Displacement amplitude of the gearbox (a) and of the fuselage (b) for cg= cf = 150 Ns/m and α0 = 26°. (*) : without DVA.

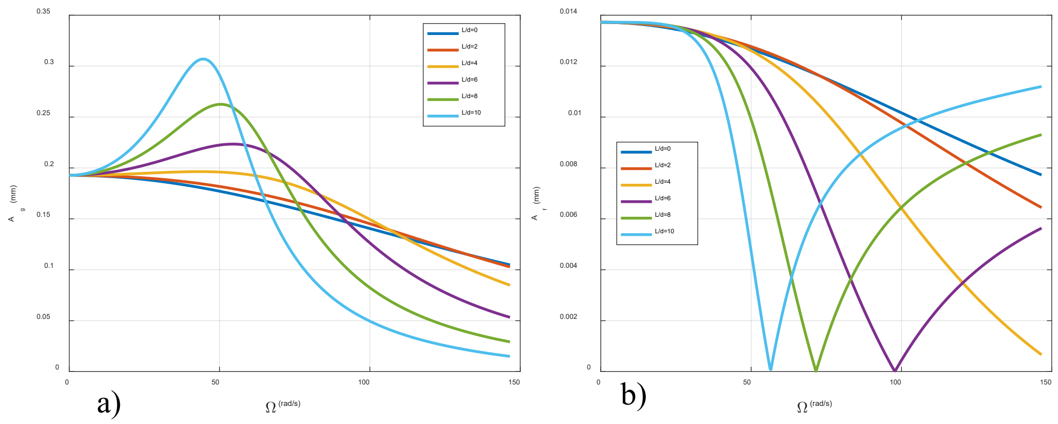

Fig. 5 Displacement amplitude of the gearbox (a) and of the fuselage (b) for cg= cf = 150 Ns/m and α0 = 0°.

The resulting dynamic response is shown on Fig. 4. The improvement is obvious concerning the maximum amplitudes, which are no longer increasing at the "resonances" and the DVA keeps its fuselage favorable functioning regimes.

Reducing the angle $\alpha_0 = 0°$ in the same conditions generates the results shown on *Fig. 5*. In this position, the DVA has maximum efficiency at lower frequencies for the fuselage, but the maximum amplitude of the gearbox increases from 0.27mm to 0.31mm at 50 rad/s. The case without DVA is represented by red stars, proving the efficacy of this device.

5. Experimental results

The experimental model was designed and manufactured according to the mechanical model shown on Fig. 1. The two masses M_f and M_g are represented by two aluminum plates, interconnected by four identical elastic springs (Fig. 6).
The base plate is supported by four rubber supports. The elastic constants of the springs were determined from the geometry of the springs (length Ls=21.4 mm, wire diameter: d=0.9 mm, coil diameter D=7.5 mm, N=5 active coils, shear modulus for steel: G = 77.2 GPa) and applying the formula from ref. *[3]*: $k = \frac{Gd^4}{8ND^3} = 3000\,N/m$. The elastic constants of the rubber supports as well as their damping coefficients were determined by the ping impact method, analyzing with a Fast Fourier Transform (FFT) the dynamic response of the base plate separately. The beam *CB* and the mass M_b (Fig. 1) are in fact in duplicate for symmetry reasons. The slider A had to be designed and manufactured using a 3D printer. The cylindrical hinges C are made from commercially available kinematic components. The excitation representing the vibrations produced by the main rotor and gearbox are simulated by two symmetrically placed DC motors, with variable rotation speed (30 – 170 rot/min) and using their intrinsic mass unbalance. The effective rotation speed was measured using a UNI-T UT373 mini digital Laser Tachometer.

Table 1

Main parameters of the mechanical model at small scale

d (mm)	L (mm)	Mg (g)	Mf (g)	Mb (g)	α_0 (°)
20	50-130	487	296.5	20.92	26

The experimental model was placed horizontally on a table under the vertical laser beam from a Polytec OFV-5000 velocimeter with an OFV-505 sensor head, frequency bandwidth 1 Hz to 1 MHz (Fig. 6). The signals from the vibrating reflecting surfaces were acquired on a Tektronix DPO4102B oscilloscope and offline analyzed using a proprietary software developed in Octave open-source high-level programming language *[14]*.

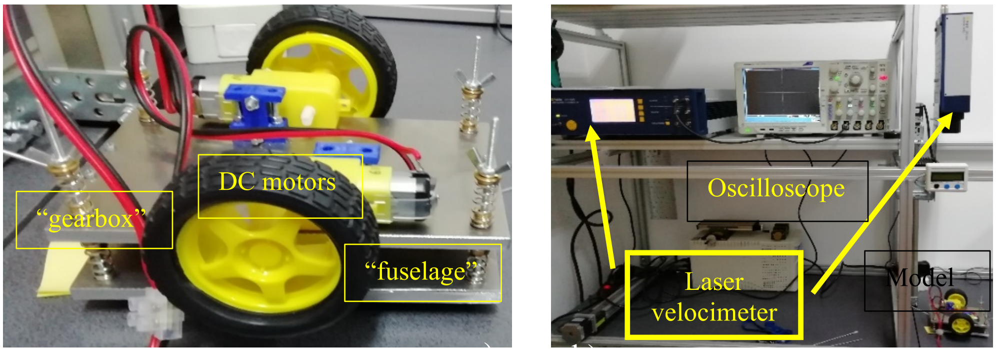

Fig. 6 Experimental model (a) and experimental setup (b)

The "ping" test on the model has led to the free vibrations spectrum (Fig. 7a) validating f_1=24 Hz and f_2=120Hz. The small peaks at 5; 33.5 Hz remain to be explained by further experiments.

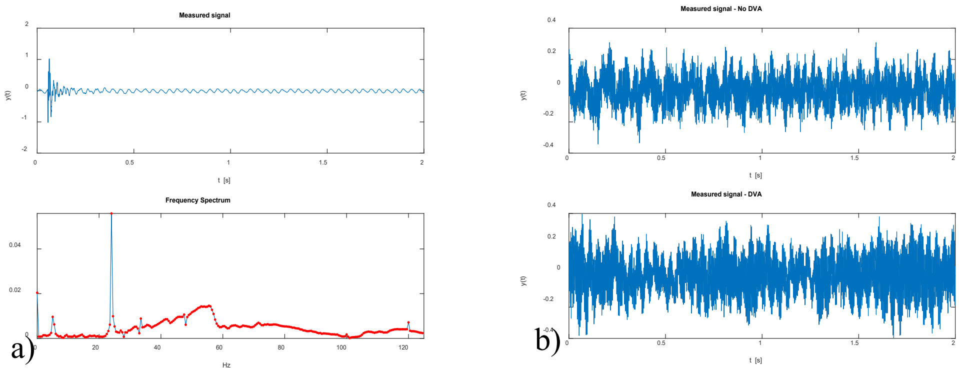

Fig. 7 Free vibrations spectrum (a) and recorded vibrations velocities up=no DVA, down = with DVA (b)

The influence of the DVA is represented on (Fig. 7b) for L/d=2.5 and 110 rot/min. The standard deviation (RMS) of the two signals is 0.09 V (no DVA) and 0.113 V (with DVA), in good agreement with Fig. 3b. The full range DVA effects are difficult to ascertain at this stage, the experiment being at low excitation frequencies.

6. Conclusions

A DVA capable of reducing the transmitted vibrations was investigated in this work. The mechanical model was studied as a non-holonomic 2-DOF mechanical system. A parametric study of DVA's position and inclination of the beam, was done using software elaborated by the authors.

An experimental stand was built to validate the numerical results. Some components were 3D printed. Using a Laser vibrometer, the vibrations velocities were determined on the two plates representing the gearbox and the fuselage. The influence of the DVA design parameters on the vibrations amplitudes were investigated, indicating optimization possibilities in practical cases. As future work, the present model could be extended, with faster motors and including mass and the flexibility of the beam used in the DVA.

Acknowledgments

The research activity of Master student Félix Tiphaine in this work has been done in accordance with the Erasmus+ student mobility framework, established between the University POLITEHNICA of Bucharest Romania and ENSAM, Cluny, France.

R E F E R E N C E S

[1] *Rades M* (2008), **Vibratii mecanice**, (Mechanical vibrations), Bucharest: Ed. Printech.

[2] *Rao SS* (2011), **Mechanical Vibrations**, Boston: Prentice Hall.

[3] Predoi MV (2011), **Vibratii Mecanice - Modele si Aplicatii in Matlab**, (Mechanical Vibrations- Models and Applications in Matlab), Bucharest: Ed. Matrix Rom.

[4] *Kelly G* (2000), **Fundamentals of Mechanical Vibrations**, Boston: Mc. Graw Hill.

[5] *Meirovitch L* (2001), **Fundamentals of Vibrations**, Boston: McGraw-Hill Higher Education.

[6] *Yuen T, Balan L, Mehrtash M* (2019), Implementation of an Absorber Design for Vibration Control in Automation Systems, *Procedia Manufacturing,* vol. 32, pp. 578-584.

[7] *Piccirillo V, Vinícius AM. Balthazar JM* (2019), Optimization of Dynamic Vibration Absorbers Based on Equal-Peak Theory, *Latin American Journal of Solids and Structures,* vol. 16, no. 4, pp. 1-22.

[8] *Shen Y, Xing Z, Yang S, Sun J* (2019), Parameters optimization for a novel dynamic vibration absorber, *Mechanical Systems and Signal Processing,* vol. 133, pp. 1-13.

[9] *Castillo-Rivera S, Tomas-Rodriguez M* (2015), Hover Flight Helicopter Modelling and Vibrations Analysis, in *Actas de las XXXVI Jornadas de Automática*, Bilbao.

[10] *Welsh WA* (2018), Chapter 27 - Helicopter Vibration Reduction, in *Morphing Wing Technologies*, Oxford, Elsevier, pp. 865-892.

[11] *Ji Z, Lin M, Chen C* (2018), Workspace computation of a tensegrity-based parallel mechanism, *U.P.B. Sci. Bull., Series D,* vol. 80, no. 1, pp. 17-28.

[12] *Nguyen TV, Petre RA, Stroe I* (2016), Application of Lagrange equations for calculus of internal forces in a mechanism, *U.P.B. Sci. Bull., Series D,* vol. 78, no. 4, pp. 15-26.

[13] *Tiphaine F, Predoi MV* (2020), "Optimization study of the vibration absorber used for a helicopter," in *Student Communication Session*, Bucharest.

[14] ***, "Octave v5.1.0 User manual (2019), GNU Free Software Foundation.